AD-A197 636

DTIC FILE COPY (4)

SECURITY CLASSIFICATION OF THIS PAGE

REPORT DOCUMENTATION PAGE

1a. REPORT SECURITY CLASSIFICATION Unclassified	1b. RESTRICTIVE MARKINGS
2a. SECURITY CLASSIFICATION AUTHORITY	3. DISTRIBUTION/AVAILABILITY OF REPORT Approved for public release and sale. Distribution unlimited.
2b. DECLASSIFICATION/DOWNGRADING SCHEDULE	
4. PERFORMING ORGANIZATION REPORT NUMBER(S) ONR Technical Report No. 7	5. MONITORING ORGANIZATION REPORT NUMBER(S)
6a. NAME OF PERFORMING ORGANIZATION University of Utah 6b. OFFICE SYMBOL (If applicable)	7a. NAME OF MONITORING ORGANIZATION
6c. ADDRESS (City, State, and ZIP Code) Department of Chemistry Henry Eyring Building Salt Lake City, UT 84112	7b. ADDRESS (City, State, and ZIP Code)
8a. NAME OF FUNDING/SPONSORING ORGANIZATION Office of Naval Research 8b. OFFICE SYMBOL (If applicable)	9. PROCUREMENT INSTRUMENT IDENTIFICATION NUMBER N00014-85-K-0712
8c. ADDRESS (City, State, and ZIP Code) Chemistry Program, Code 1113 800 N. Quincy Street Arlington, VA 22217	10. SOURCE OF FUNDING NUMBERS PROGRAM ELEMENT NO. / PROJECT NO. / TASK NO. / WORK UNIT ACCESSION NO

11. TITLE (Include Security Classification)
Properties of Electrochemically Generated Poly(p-Phenylene)

12. PERSONAL AUTHOR(S)
K. Ashley, D. B. Parry, J. M. Harris, and S. Pons

13a. TYPE OF REPORT	13b. TIME COVERED	14. DATE OF REPORT (Year, Month, Day)	15. PAGE COUNT
Technical	FROM 9/87 TO 7/88	July 15, 1988	35

16. SUPPLEMENTARY NOTATION

17. COSATI CODES		
FIELD	GROUP	SUB-GROUP

18. SUBJECT TERMS (Continue on reverse if necessary and identify by block number)
Conducting polymers, Raman spectroscopy of surface species.

19. ABSTRACT (Continue on reverse if necessary and identify by block number)

Attached.

DTIC ELECTE JUL 27 1988 S D H

20. DISTRIBUTION/AVAILABILITY OF ABSTRACT ☒ UNCLASSIFIED/UNLIMITED ☐ SAME AS RPT ☐ DTIC USERS	21. ABSTRACT SECURITY CLASSIFICATION Unclassified
22a. NAME OF RESPONSIBLE INDIVIDUAL	22b. TELEPHONE (Include Area Code) / 22c. OFFICE SYMBOL

DD FORM 1473, 84 MAR 83 APR edition may be used until exhausted
All other editions are obsolete

SECURITY CLASSIFICATION OF THIS PAGE

OFFICE OF NAVAL RESEARCH

Contract N00014-85-K-0712

R&T Code 413a001---01
Replaces Old Task #056-123

Technical Report No. 7

Properties of Electrochemically Generated Poly(p-Phenylene)

Prepared for publication in Electrochim. Acta

by

K. Ashley, D. B. Parry, J. M. Harris, and S. Pons

Department of Chemistry
University of Utah
Salt Lake City, UT 84112

July 15, 1988

PROPERTIES OF ELECTROCHEMICALLY GENERATED POLY(p-PHENYLENE)

Kevin Ashley

Department of Chemistry
San Jose State University
San Jose, California 95192

Diane B. Parry, Joel M. Harris, and Stanley Pons*

Department of Chemistry
University of Utah
Salt Lake City, Utah 84112

Douglas N. Bennion, Rodney LaFollette, and Jeffery Jones

Department of Chemical Engineering
Brigham Young University
Provo, Utah 84602

and

Edward J. King

Department of Biology
University of Utah
Salt Lake City, Utah 84112

*To whom correspondence should be addressed

ABSTRACT

Poly(p-phenylene) (PPP) electrodes formed by anodic oxidation of biphenyl in acetonitrile solutions were examined. As a cell, we observe generally high discharge current densities and rapid discharge rates. PPP electrochemistry and cell performance were found to depend significantly on the nature of the supporting electrolyte present during electrosynthesis and doping. These electrodes were also found to catalyze O_2 reduction. Raman and scanning electron microscopic results are also presented.

INTRODUCTION

Organic conducting polymers such as poly(p-phenylene) (PPP) have high potential for numerous commercial applications in sensor and battery technologies, electrochromic devices, and in semiconductors (1). The discovery that conjugated polymers may be converted to highly conducting materials by intercalation of electron donors and acceptors has stimulated a large amount of research activity in recent years. Poly(p-phenylene) has historically been synthesized principally by various homogeneous chemical means (2-9). Subsequently acceptor or donor doping is usually accomplished by exposure of the insulating undoped polymer to charge transfer agents (such as AsF_5) in the gaseous state (1, 10). Electrochemical doping of conductive polymers has been employed less frequently (10c, 11-13). This method, however, offers an advantage over chemical doping in that the degree of dopant intercalation may be more easily controlled and monitored. Polymers of desired conductivities may therefore be obtained with greater ease and speed than by homogeneous chemical means.

Electrolytic synthetic methods for PPP have been reported; most of these have involved the electrolysis of benzene and substituted aromatic precursors which form the polymer by anodic oxidation (14-18). Severe chemical conditions have been required in most cases in order to effect polymer formation. The recent demonstration that PPP can be electroformed from dissolved biphenyl under mild anodic conditions (18-20) has provided a more convenient electrochemical means for synthesis of the polymer. Besides being less toxic than benzene, biphenyl oxidation only requires the use only of aprotic solvents; this is more attractive than HF and liquid SO_2, which are required for benzene oxidation. Furthermore, this method yields poly(p-phenylene) with a generally longer chain length and a lesser degree of cross-linking than PPP electroformed from benzene.

In this paper we have studied various doped PPP films formed in the presence of different supporting electrolytes. Both n- and p-type PPP-modified Pt electrodes were formed. The polymers

were characterized by Raman spectroscopy, scanning electron microscopy, and electrochemistry.

EXPERIMENTAL

A. Materials and Electrochemistry

Anhydrous acetonitrile (Aldrich, water content <0.005 %) was stored over alumina (Woelm Super I). Solutions were degassed with dry helium, argon, or nitrogen prior to experiments. Exposure to air was minimized, and experiments were conducted in He, Ar, or N_2 atmosphere. For voltammetric experiments the reference electrode was 0.01 M $AgNO_3$ in 0.10 M electrolyte/CH_3CN; all potentials in the voltammetric experiments are reported vs. Ag/Ag^+.

Lithium hexafluoroarsenate (electrochemical grade) was obtained from USS Agrichemicals; lithium tetrafluoroborate came from Alfa, and lithium perchlorate was purchased from Smith Chemical Co. The tetraalkylammonium salts tetraethyl-, tetrapropyl-, and tetraoctylammonium perchlorates (TEAP, TPAP, and TOAP, respectively), and tetramethylammonium tetrafluoroborate (TMAF), were obtained from Fluka. Tetraethylammonium tetrafluoroborate (TEAF) was obtained from Aldrich, and tetrabutylammonium tetrafluoroborate (TBAF) came from Chem-Biochem Research. All electrolytes (with the exception of $LiAsF_6$) were recrystallized and stored in a vacuum oven (>24 h, 75 °C) before use.

The electrochemical equipment (potentiostat and waveform generator) was provided by JAS Instrument Systems, Inc. Platinum working electrodes were 6 mm diameter polished disks, as per ref. (21); secondary electrodes consisted of platinum foil. The electrochemical cell design has been described previously (21). For three-electrode experiments, a Luggin capillary reference was employed. For two-electrode studies, the working electrodes were placed facing one another and separated by approximately 1 mm. Current-potential curves were recorded on a digital plotter (Hewlett-Packard model 7015B), and current-time plots were stored on a digitizing oscilloscope

(LeCroy model 9400).

PPP electrodepositions were carried out in acetonitrile solutions; the concentrations of biphenyl and supporting electrolyte were 5.0 mM and 0.10 M, respectively.

B. Raman Spectroscopy

Single scan Raman spectra were obtained from PPP-modified Pt disk electrode surfaces using a Spex Ramalog 4 double monochromator equipped with an RCA C31034 water-cooled photomultiplier detector. Spectra were recorded on a plotter (Houston Instruments model 2000). Excitation radiation was provided by an argon ion laser (Spectra-Physics model 165-09). A Claasen filter was employed for plasma line rejection. The power at the sample was 100 mW and the excitation wavelength was 488.0 nm.

C. Scanning Electron Microscopy

After preparation, PPP-modified Pt electrodes were allowed to dry in air. Electrodes were then mounted on aluminum specimen stubs by use of copper tape and conductive silver paint (Pelco, Inc.), and sputter-coated with 15-20 nm of gold or gold:palladium (60:40) in a Denton Desk instrument. Films were examined in a Hitachi S-450 scanning electron microscope operated at 25 or 30 KV at a working distance of 5 mm. Micrographs were obtained on Polaroid 55 P/N film.

RESULTS AND DISCUSSION

A. Electrodeposition

Figure 1 shows a typical cyclic voltammogram for the formation of PPP on a platinum electrode from a solution containing tetra-n-butylammonium tetrafluoroborate (TBAF) as supporting electrolyte. The anodic oxidation of biphenyl is chemically irreversible, and during the potential sweep to positive potentials a color change due to polymer deposition on the electrode

surface is observed at about +1.6 V (vs. Ag/Ag^+). The initial color of the film is brassy, and, at higher potentials, the color becomes dark brown to black. On the second and subsequent scans the current is markedly lower than on the initial scan, and no further color change on the electrode is observed. This suggests that the film formed during the first cycle is somewhat passivating and prevents further biphenyl oxidation.

Cyclic voltammetry of PPP electrodeposition in the presence of other tetrafluoroborate electrolytes (lithium tetrafluoroborate, tetra-n-methylammonium tetrafluoroborate (TMAF), and tetra-n-ethylammonium tetrafluoroborate (TEAF)) mimicked the voltammetric results obtained in $TBAF/CH_3CN$ solutions; the anodic current on the first scan was always high, due to diffusion controlled biphenyl oxidation (19b, 22). On successive scans the current was attenuated significantly.

However, different voltammetric characteristics were observed during PPP film electroformation in the presence of perchlorate and hexafluoroarsenate electrolytes (Figure 2). The current on the first scan is high, and on the following scan the current decays to about one third that of the initial scan, reaching a constant value: the current is relatively unchanged on further cycling. During the first cycle a brassy-colored film is formed on the Pt surface which darkens with subsequent scans. These results indicate that continuous electrochemical PPP deposition can be facilitated in perchlorate and hexafluoroarsenate electrolyte systems; however, in tetrafluoroborate electrolytes, only a limited amount of polymer can be electrodeposited on the Pt electrode. Voltammetry indicates that there is adsorption of product, followed by continued oxidation of the solution biphenyl. This is evidenced by shoulders prior to the main wave (seen in hexafluoroarsenate, or the shoulders and double peaks observed in perchlorate.

Similar results were obtained for PPP electrodeposited by potential pulse techniques. The potential was square-wave modulated from a base potential where no faradaic reaction occurred to a potential at which anodic oxidation of biphenyl occurs; the potential modulation frequency was

0.5 Hz. Figure 3 shows the resulting current-time behavior during polymer deposition in TBAF solution. Other tetrafluoroborate electrolytes ($LiBF_4$, TMAF, TEAF) gave nearly identical chronoamperometric behavior. The charge passed on the initial pulse is high, but decays rapidly on subsequent pulses. Upon reversal of the potential pulse, a very small charge is observed, demonstrating the irreversibility of the electrochemical reaction. During the potential modulation, the dark deposit is observed almost immediately after initiation of the modulation sequence. The charge observed during application of pulses to positive potentials is seen to decay to near zero after a short time. Only a limited amount of polymer film can be made to electrodeposit in this electrolyte system, again indicating that a passivating film is formed.

Chronoamperometry from PPP pulse modulation electrodeposition in perchlorate and hexafluoroarsenate electrolytes again behaved differently. Figure 4 illustrates the chronoamperometry for PPP deposition in $LiClO_4$ electrolyte; similar results were obtained in other perchlorate electrolytes (TEAP, TPAP, TOAP). The charge passed on the first pulse is quite high, and decays somewhat on subsequent pulses. However, the degree of decay is not as appreciable compared to the case of PPP electrodeposition in TBAF. After the initial potential pulse the current decay is extremely slow, and the total integrated current is nearly constant with repeated pulsing. Biphenyl oxidation is irreversible in this electrolyte (as in TBAF), as evidenced by the small charge passed observed upon reversal of the potential step. A brassy color due to deposition of the PPP film on the Pt electrode surface is observed almost immediately following initiation of the potential modulation program. The film color is seen to darken gradually during continuous, repetitive pulsing, and a dark brown to black film is ultimately obtained after about 20 min. These observations, coupled with the chronoamperometric data, indicate that the polymer, when electrochemically deposited in the presence of perchlorate or hexafluoroarsenate electrolytes, is <u>not</u> passivating to further film electrodeposition. On the contrary, continuous film buildup can be facilitated in perchlorate and hexafluoroarsenate electrolytes, in contrast to the case of

electrodeposition in tetrafluoroborate electrolytes.

Unlike polymer films formed in tetrafluoroborate and perchlorate electrolytes, PPP films electroformed in $LiAsF_6$ solutions could be deposited continuously at a high applied potential; repeated potential pulsing was not required to enable continued film buildup after an initial potential pulse. In $LiAsF_6$, the potential could be held at a high anodic potential indefinitely, and the observed current (due to biphenyl oxidation) remained appreciable for a very long time period (at least 1 min). Continued film deposition was observed at the Pt electrode during the application of a long potential pulse to +1.80 V. PPP's formed in perchlorate and tetrafluoroborate electrolytes, however, required repeated pulsing in order to facilitate continued film growth.

It should be pointed out that PPP, when formed as described above, is simultaneously p-doped (19b, 23); it is this doping process that is responsible for the polymer's conductivity, which may exceed 100 S/cm if electrodeposited in the presence of AsF_6^-. PPP conductivities are less for polymers formed electrochemically from biphenyl in other electrolytes (BF_4^-, ClO_4^-). Polymer film thicknesses were estimated by measuring the charge passed during the electrodeposition, and confirmed by SEM.

Conductivities of the films were measured by a 4-point probe method and were found to be in the ranges 10-100 S/cm (hexafluoroarsenate doped), 1-10 S/cm (tetrafluoroborate doped), and 0.1-1 S/cm (perchlorate doped).

B. Film Voltammetry

The characteristic voltammetry of PPP films grown potentiostatically from biphenyl in TBAF electrolyte is shown in Figure 5. Figure 5a illustrates the voltammetry at positive potentials (vs. Ag/Ag^+). The polymer is oxidized quasi-reversibly at about +0.8 V, and a large capacitative component is observed upon switching (24). PPP donor doping occurs at these anodic potentials, and undoping can be achieved by sweeps to more negative potentials. The voltammetry is unchanged for >100 repeated scans, thus demonstrating the stability of the conducting polymer.

In Figure 5b we see the voltammetric behavior of the film at negative potentials in TBAF/CH_3CN solution. n-doping occurs at about -1.9 V, where PPP is reduced; the small cathodic wave at approximately -1.3 V is due to trace oxygen present in the reaction mixture.

It is interesting to note that O_2 is reduced catalytically at a PPP-modified electrode (Figure 6). On platinum, the $O_2/O_2^{\cdot}$ redox couple is quasi-reversible: the peak potential (E_p) for O_2 reduction on bare Pt occurs at -1.60 V and the peak separation between the O_2 reduction peak and the superoxide oxidation peak (on the return anodic sweep) exceeds 800 mV. However, on a PPP-modified surface, O_2 reduction occurs at less negative potentials than on Pt, and the peak separation is less than 300 mV (Figure 6). The electrocatalytic properties of PPP-modified electrodes prepared from biphenyl oxidation has been investigated previously for other redox couples (19).

Figure 7 shows the characteristic voltammetry of a PPP film formed in solution which contained TEAP as supporting electrolyte. For films formed from perchlorate electrolytes, the voltammetry was found to be dependent on the supporting electrolyte cation (19b, 23). The degree of film oxidation increased as the molecular size of the cation was increased. This is thought to be related to differences in polymer morphologies caused by cations of varied size which co-deposit into the conductive polymer matrix to some extent (along with electrolyte anions which cause p-doping). Specific studies on the mechanistic nuances brought about by supporting electrolytes of different nature during the conducting polymer electrodeposition process are currently underway, and the results will appear elsewhere.

Although the TEAP/PPP polymer is less electroactive than PPP electroformed in TBAF solution, it was found that cathodic oxygen reduction at a TEAP/PPP film is catalytic, just as in the TBAF/PPP film. However, the oxygen wave at a TEAP/PPP polymer was lower in magnitude than the voltammetric wave at a TBAF/PPP film (for an O_2 saturated solution), suggesting much lower film conductivity for the perchlorate doped polymer. As a general rule PPP films cast in the

presence of tetrafluoroborate electrolytes were more electroactive than films cast in perchlorate solutions; a notable exception to this was TOAP/PPP polymers (19b), which gave high, though irreversible, oxidative currents. This was determined to be related to the extent of film doping occurring during the electrodeposition, as evidenced by substantial potential differences (in blank electrolytes) between p-doped PPP's electrosynthesized in the different electrolyte systems. For example, a potential difference of nearly a volt was measured (in an electrolyte solution: 0.10 M $LiClO_4/CH_3CN$) between PPP-modified electrodes prepared in TBAF and TEAP solutions (0.10 M in electrolyte), respectively.

PPP films electroformed in perchlorate electrolytes exhibit irreversible oxidation and reduction waves (Figure 7). It is possible that polymer phase changes occur upon oxidation or reduction, and this is responsible for the electrochemical irreversibility. Furthermore, it was noticed (for perchlorate/ PPP polymers) that on succeeding anodic cycles (following the initial scan to positive potentials) the current magnitude was attenuated significantly, and ultimately disappeared after 15-20 scans. Again, these observations may be related to irreversible phase changes caused by oxidation of the conductive polymer. Also, during anodic sweeps, upon potential switching, little or no capacitative effect is observed in the perchlorate/PPP film electrochemistry (Figure 7a). This is in contrast with the results presented above for tetrafluoroborate/ PPP films. These results may be related to the lower conductivities (due to less extensive donor doping) and much lower surface areas of the perchlorate doped polymers compared with tetrafluoroborate doped films.

Voltammetric results, obtained in blank electrolyte (no biphenyl present in solution), are shown in Figure 8 for a PPP-modified electrode electrochemically synthesized from biphenyl in $LiAsF_6/CH_3CN$ electrolyte. This polymer is oxidized at a lower potential than PPP's doped with tetrafluoroborate and perchlorate electrolytes, and a significant capacitative component is observed upon potential switching during anodic scans (Figure 8a). Recall that high capacitances were observed in tetrafloroborate-doped films as well (see above). The voltammetry was essentially

unchanged after several hundred scans, indicating high film stability. The $LiAsF_6$/PPP film is reduced at a more negative potential than tetrafluoroborate- and perchlorate-doped PPP's (Figure 8b). The reduction wave is irreversible; PPP films doped with tetrafluoroborate and perchlorate also gave irreversible reduction waves (Figures 6b, 7b) . Scans to very high positive potentials (greater than +1.5 V) caused breakdown of the polymer film, as indicated by a lack of electroactivity on subsequent anodic sweeps. In tetrafluoroborate- and perchlorate-doped polymers this electrochemical breakdown process existed, but was less pronounced.

The hexafluoroarsenate doped polymer was highly conductive, and oxygen reduction at this film was found to be electrocatalytic, as in tetrafluoroborate- and perchlorate-doped polymers. The electroactivity of the hexafluoroarsenate-doped PPP is similar to that of polypyrrole (12, 13, 24, 25), and it is interesting to note that PPP doping with AsF_6^- anion lowers the oxidation potential of the conducting polymer in comparison with BF_4^- and ClO_4^- doped PPP's.

An electrochromic effect was observed during the pulse PPP deposition process; this phenomenon has been previously observed in other electrochemically synthesized PPP films (20). The film color changed from a light brassy color at neutral potential to dark green when oxidized, and the color change was fast (rise time < 1 ms) and reversible with potential pulsing. This effect was most noticeable in thin polymer films (<0.2 microns); thick films (>0.5 microns) were very dark to begin with, so changes in color caused by changes in electrode potential were not so evident.

Effects of various media on the anodic fabrication of PPP films on Pt, such as water content, solvent, and the nature of the background electrolyte, have been examined in nonaqueous solvents, including CH_3CN (20). It was found that electrodeposition in perchlorate electrolyte gave predominately insulating films, while electroformation from tetrafluoroborate electrolyte yielded conductive polymer deposits; our results are in agreement with these findings. However, in contrast to the results of ref. (20), we found that PPP films electrochemically polymerized in acetonitrile solutions were for the most part homogeneous and strongly adherent on the electrode surface,

regardless of the supporting electrolyte employed. One exception was very thick hexafluoroarsenate-doped films, which tended to flake off the electrode surface to some extent. It is thought that some film breakdown occurred on successive potential pulsing during electrodeposition in $LiAsF_6/CH_3CN$ solution, and this caused a degree of film cracking and flaking. Medium effects have been observed in inorganic conducting polymers, for example poly(vinylferrocene) (26), so the influence of electrolyte is not restricted to organic conducting polymers.

It may be that the mechanism of PPP electrochemical polymerization is similar to that of polypyrrole electrodeposition (27), since (a) the voltammetric characteristics of the PPP electrosynthesis process are very similar to those of polypyrrole electroformation (19), and (b) the transient spectroelectrochemical response during film electrodeposition is similar in both cases, which indicates that the rate determining processes are similar (19b,22). The PPP electropolymerization process may be initiated by electrolyte radicals present in small amounts near the electrode/solution interface (28), or by coupling of biphenyl radicals. Ion pairing interactions may play a role in determining the rate of the electrochemical polymerization, with the nature of the supporting electrolyte having a strong effect on the electrocatalysis. Kinetic and mechanistic studies of PPP electrochemical polymerizations in different supporting electrolytes are currently being investigated.

C. Discharge Characteristics

Simple PPP electrolytic cells were constructed in the following manner. Two PPP-modified Pt electrodes were placed in the appropriate electrolyte solution. The electrodes mounted facing one another and were separated by approximately 1 mm. A potential was then applied between the two electrodes for a fixed time period (19). Electrolyte ions were thereby intercalated into the respective films. Following the charging period, the cell was deliberately shorted, and the discharge

curve obtained as described.

Typical discharge currents for various PPP cells are presented in Table I. Each cell was charged at 4 V for 20 min, and then discharged at a measured open circuit potential. High discharge current densities were observed for PPP cells prepared in most of the electrolytes used, and discharge times were all under 100 ms. $LiClO_4$ and $LiBF_4$ cells gave significantly lower discharge currents than the other PPP cells shown in the table. The LiAsF6-PPP cell yielded a high discharge current, in contrast to the other two lithium electrolyte-PPP cells studied. Also, this cell demonstrated a significant plateau current (about 20 mA/cm^2) at long times, following the initial peak discharge current. No other system showed appreciable plateau currents of this kind. Some dependence on the electrolyte cation present in the cell system is observed in Table I. The major differences due to electrolyte cation appear between lithium and tetraalkylammonium salts (of both perchlorate and tetrafluoroborate electrolytes).

We view the charge-discharge process as a combination of quasi reversible cation radical formation and supporting electrolyte anion migration into and out of the oxidized film form of the PPP film, and supporting electrolyte cation migration in and out of the reduced film. Ever. ually, the reduced film is converted into a mechanically unstable form that is unable to contain enough electrolyte to maintain a cell characteristic. It is possible that another type of anode (lithium metal, etc.) would therefore enhance the overall cell performance.

Table II summarizes the recorded open circuit cell potentials for various PPP cells, both before and after cell discharge. Also included in Table II is a qualitative measure of the cell stability, as indicated by the relative rate of potential decay at open circuit. Instabilities were found to be due primarily to the instability of the anode, or n-doped PPP electrode. The following trend was observed: the larger the electrolyte cation molecular size, the more unstable the n-type electrode. If a large tetraalkylammonium cation was used for n-doping, the polymer comprising the anode broke down easily under the mechanical strain of the charge-discharge process. This was

evidenced by a flaking off of the n-doped polymer from the platinum electrode surface following charge-discharge cycles. By measuring the potential difference between a silver reference electrode and each of the two electrodes comprising the PPP cell, it was observed that the rate of potential decay of the anode greatly exceeded that of the cathode in all cases. Furthermore, the rate of anode decay was fastest for electrolytes with large tetraalkylammonium cations and slowest for systems with lithium ion as the n-dopant. Calculated charge and energy densities for the various cells are presented in Table III.

p-doped PPP films were found to be quite stable in all cases, with hexafluoroarsenate-intercalated PPP yielding the slowest rate of potential decay and perchlorate-doped polymer showing the fastest rate of decay. p-type films did not flake off the Pt base electrode as easily as did the n-type films after long charging and recharging periods. The most stable cell was the $LiAsF_6$/PPP system, which held a potential of greater than 2 V for over 12 h. Some of the other systems studied gave somewhat higher initial (peak) discharge currents (Table I), but the $LiAsF_6$/PPP cell was found to be more easily rechargeable (i.e., minimum film breakdown during cell charging) and had the longest lifetime of the PPP cells investigated.

A practical consequence of the instability of the n-doped PPP electrode in potential cell applications may be the use of a lithium anode with a p-type PPP cathode (18b); the practicality of an analogous Li-PP cell has also been demonstrated (29). Furthermore, PPP-alkali metal composites have been shown to have advantages as possible cell materials (30), and electrochemical fabrication of such composites is being investigated.

D. Raman Spectroscopy

The Raman spectrum of a PPP film formed electrochemically in 0.10 M TBAF/CH_3CN is shown in Figure 9; the excitation wavelength was 4880 Å. Bands appear at about 1600, 1330, 1280, and 910 cm^{-1}; the results are consistent with a planar molecular configuration (31). Undoped PPP

(formed by the Kovacic synthesis method, ref. (2)) gives rise to Raman bands near 1600, 1280, and 1220 cm^{-1} (32). The observed bands are consistent with those obtained for doped PPP. The band near 1330 cm^{-1} is attributed to the B_{12} Raman mode (31b); the bands near 1280 and 1600 cm^{-1} are assigned to A_g modes (33). In the doped PPP sample (Figure 9), the absence of a Raman feature at about 1250 cm^{-1}, which would be due to the presence of short phenylene oligomers (34), is indicative of a long chain length. A low degree of crosslinking is also suggested by the close agreement of the spectral results with a theoretical model based on a planar PPP configuration (34).

E. Scanning Electron Microscopy

Scanning electron microscopy was employed in an effort to examine the morphologies of PPP films grown at different growth rates and in different electrolytes. Figure 10 shows a scanning electron micrograph of a PPP film electrodeposited (from biphenyl) in 0.10 M $LiClO_4$ at +1.8 V vs. Ag/Ag^+. The observed cracks were found to arise after exposure of the film to air after polymer fabrication. The whitish globules in the micrograph are $LiClO_4$ crystals on the surface of the polymer film. A micrograph of a PPP film electroformed in 0.10 M TBAF at +1.8 V is shown in Figure 11. We note the significant morphological differences between the polymer films formed in perchlorate and tetrafluoroborate electrolytes. Figure 12 shows SEM of a PPP film prepared in 0.10 M $LiAsF_6$. The morphology of this film differs from that of films formed in BF_4^- and ClO_4^- electrolytes. PPP morphologies are obviously dependent on the nature of the supporting electrolyte present during electrosynthesis, and this may be responsible for the observed differences in electrochemical properties.

Figure 13 shows the effect of polymer growth rate on the PPP morphology. Two phases seem to predominate: a "smooth" phase at low growth rate (Figure 13a) and a "globular" phase prevalent in films grown at high rate (Figure 13c). For polymers grown at intermediate rates

(Figure 13b), areas of both smooth and globular textures resulted. Analogous observations were made for PPP films of varied thickness: smooth morphology was observed in thin (<0.2 micron) polymers, while an uneven globular appearance prevailed in thick (>1.0 micron) layers; both smooth and globular regions were seen in PPP films of intermediate thickness (about 0.5 micron).

The globular phase appears to be related to high conductivity. Films formed at high electrodeposition rates were in general more electroactive than films grown at low rates; such an observation has been made for electrosynthesized polymer (34). PPP's prepared in BF_4^- and AsF_6^- electrolytes demonstrated a high degree of globular morphology, unlike PPP formed in the presence of ClO_4^-, which gave rise to a smooth film. Recall that PPP's formed in perchlorate electrolytes are predominately insulating in nature (19, 20), while polymers prepared in the presence of tetrafluoroborate and hexafluoroarsenate demonstrate reasonably high conductivity (1a, 18-20). It is possible that this globular polymer phase may allow for rapid mass transport of electrolyte through the polymer film, while the smooth homogeneous phase impedes electrolyte transport. Conducting PPP polymers with large surface areas, such as BF_4^- and AsF_6^- doped films, appear to provide the most desirable high mass transport characteristics.

Acknowledgment

We thank the Office of Naval Research for support of this work. KA thanks the San Jose State University Foundation for a research grant.

REFERENCES

1. (a) J. E. Frommer and R.R. Chance, in Encyclopedia of Polymer Science and Engineering, Vol. 5, 2nd ed.; M. Grayson and J. Kroshwitz, Eds. Wiley: New York, 1986. (b) R. L. Elsenbaumer and L. W. Shacklette, in Handbook of Conducting Polymers; T. Skotheim, Ed. Marcel Dekker: New York, 1986. (c) R. H. Baughman, J. L. Bredas, R. R. Chance, R.L. Elsenbaumer, and L. W. Shacklette, **Chem. Rev. 82**, 209 (1982).

2. (a) P. Kovacic and A. Kyriakis, **Tetrahedron Lett.** 467 (1962). (b) P. Kovacic and A. Kyriakis, **J. Am. Chem. Soc. 85**, 454 (1963). (c) P. Kovacic and M. B. Jones, **Chem. Rev. 87**, 375 (1987). (d) P. Kovacic and J. Oziomek, **J. Org. Chem. 29**, 100 (1964). (e) P. Kovacic and R. J. Hopper, **J. Polym. Sci. 4**, 1445 (1966). (f) S. K. Taylor, S.G. Bennett, I. Khoury, and P. Kovacic, **J. Polym. Sci., Polym. Lett. Ed. 19**, 85 (1981).

3. (a) T. Yamamoto and A. Yamamoto, **Chem. Lett.** 353 (1977). (b) T. Yamamoto, Y. Hayashi, and A. Yamamoto, **Bull. Chem. Soc. Jpn. 51**, 2091 (1978).

4. (a) J. F. Fauvarque, M. A. Petit, F. Pfluger, A. Jutand, C. Chevrot, and M. Troupel, **Makromol. Chem., Rapid Commun. 4**, 455 (1983). (b) G. Froyer, F. Maurice, J. Y. Goblot, J.F. Fauvarque, M. A. Petit, and A. Digua, **Mol. Cryst. Liq. Cryst. 118**, 267 (1985). (c) J. F. Fauvarque, A. Digua, A.; M. A. Petit, and J. Savard, **Makromol. Chem. 186**, 2415 (1985).

5. A. A. Berlin, **J. Polym. Sci. 55**, 621 (1961).

6. T. W. Campbell and R. N. McDonald, **J. Org. Chem. 24**, 730 (1959).

7. J. A. Cade and A. Pilbeam, **J. Chem. Soc.** 114 (1964).

8. M. Jozefowicz, **Bull. Soc. Chim. France** 2036 (1963).

9. D. G. H. Ballard, A. Courtis, I. M. Shirley, and S. C. Taylor, **J. Chem. Soc., Chem. Commun.** 954 (1983).

10. (a) L. W. Shacklette, H. Eckhardt, R.R. Chance, G. G. Miller, D. M. Ivory, and R. H. Baughman, **J. Chem. Phys. 73**, 4098 (1983). (b) D. M. Ivory, G. G. Miller, J. M. Sowa, L. W. Shacklette, R. R. Chance, and R. H. Baughman, **J. Chem. Phys. 71**, 1506 (1979). (c) L. W. Shacklette, R. R. Chance, D. M. Ivory, G. G. Miller, and R. H. Baughman, **Synth. Met. 1**, 307 (1979).

11. (a) P. J. Nigrey, A. G. MacDiarmid, and A. J. Heeger, **J. Chem. Soc., Chem. Commun.** 594 (1979). (b) D. MacInnes, Jr.; M. A. Drury, P. J. Nigrey, D. P. Nairns, A. G. MacDiarmid, and A. J. Heeger, **J. Chem. Soc., Chem. Commun.** 316 (1981).

12. M. Josowicz, J. Janata, K. Ashley, and S. Pons, **Anal. Chem. 59**, 253 (1987).

13. K. K. Kanazawa, A. F. Diaz, M. T. Krounbi, and G. B. Street, **Synth. Met. 4**, 119 (1981).

14. A. F. Shepard and B. F. Dunnels, **J. Polym. Sci. 4**, 511 (1966).

15. (a) I. Rubinstein, **J. Polym. Sci. 21**, 3035 (1983). (b) I. Rubinstein, **J. Electrochem. Soc. 130**, 1506 (1983).

16. T. Osa, A. Yildiz, and T. Kuwana, **J. Am. Chem. Soc. 91**, 3994 (1969).

17. (a) D. G. Walker and N. E. Wisdom, U.S. Pat. 3,437,569 (1969). (b) N. E. Wisdom, U.S. Pat. 3,437,570 (1969).

18. (a) M. Satoh, M. Tabata, K. Kaneto, and K. Yoshino, **J. Electroanal. Chem. 195**, 203 (1985). (b) M. Satoh, M. Tabata, K. Kaneto, and K. Yoshino, **Jpn. J. Appl. Phys. 25**, L73 (1986). (c) M. Tabata, M. Satoh, K. Kaneto, and Y. Katsumi, **J. Phys. C: Solid State Phys. 19**, L101 (1986). (d) M. Satoh, M. Tabata, F. Uesugi, K. Kaneto, and K. Yoshino, **Synth. Met. 17**, 595 (1987).

19. (a) J. F. McAleer, K. Ashley, J. J. Smith, S. Bandyopadhyay, J. Ghoroghchian, E. M. Eyring, S. Pons, H. B. Mark, Jr., and G. Dunmore, **J. Mol. Electron. 2**, 183 (1986). (b) K. Ashley, **Ph.D. Dissertation**, University Of Utah, USA, 1987.

20. S. Aeiyach, J. E. Dubois, and P. C. Lacaze, **J. Chem. Soc., Chem. Commun.**, 1668 (1986).

21. K. Ashley and S. Pons, **Trends Anal. Chem. 5**, 263 (1986).

22. E. M. Genies, G. Bidan, and A. F. Diaz, **J. Electroanal. Chem. 149**, 101 (1983).

23. K. Ashley, S. Pons, and M. Fleischmann, in preparation.

24. S. W. Feldberg, **J. Am. Chem. Soc. 106**, 4671 (1984).

25. T. A. Skotheim, S. W. Feldberg, and M. B. Armand, **J. Phys. (Paris) C3**, 270 (1983).

26. G. Inzelt and L. Szabo, **Electrochim. Acta 31**, 1381 (1986).

27. M. L. Marcos, I. Rodriguez, and J. Gonzalez-Velasco, **Electrochim. Acta 32**, 1453 (1987).

28. S. N. Bhadani and G. Parravano, in Organic Electrochemistry, 2nd ed. M. M. Baizer and H. Lund, Eds. Marcel Dekker: New York, 1983; Ch. 31, and references therein.

29. S. Panero, P. Prosperi, F. Bonino, B. Scrosati, A. Corradini, and M. Mastragostino, **Electrochim. Acta 32**, 1007 (1987).

30. T. R. Jow, L. W. Shacklette, M. Maxfield, and D. Vernick, **J. Electrochem. Soc. 134**, 1730 (1987).

31. (a) D. Racovic, I. Bozovic, S. A. Stepanyan, and L. A. Gribov, **Solid State Commun. 43**, 127 (1982). (b) I. Bozovic and D. Racovic, **Phys. Rev. B 32**, 4235 (1985).

32. S. Krichene, S. Lefrant, Y. Pelous, G. Froyer, M. Petit, A. Digua, and J. F. Fauvarque, **Synth. Met. 17**, 607 (1987).

33. S. Krichene, J. P. Buisson, and S. Lefrant, **Synth. Met. 17**, 589 (1987).

34. D. Racovic and I. Bozovic, **Synth. Met. 17**, 613 (1987).

35. S. Panero, P. Prosperi, and B. Scrosati, **Electrochim. Acta 32**, 1461 (1987).

Table I. Discharge behavior of PPP cells prepared in various electrolyte media. Cells were charged at 4.0 V for 20 min prior to discharge through 10 ohms. Solutions 0.10 M in supporting electrolyte/CH_3CN.

Dopant electrolyte	Cell potential at discharge (V)	Peak discharge current density (mA/cm^2)	Characteristic discharge time (ms)
$LiAsF_6$	2.5	175	60
$LiClO_4$	2.0	50	40
TEAP	1.5	185	45
TOAP	1.0	205	35
$LiBF_4$	2.0	65	50
TEAF	2.0	125	45
TBAF	2.2	180	30

Table II. Recorded cell potentials prior to and following cell discharge through 10 ohms for PPP cells fabricated in varied electrolyte media. Also listed are relative rates of cell potential decay: "fast" rate of decay (about 1 V/min); "moderate" (about 0.2 V/min); "slow" (about 0.05 V/min). Cell electrolyte concentrations were 0.10 M in CH_3CN.

Cell electrolyte	Potential before discharge (V)	Rate of cell potential decay	Potential after discharge (V)
$LiAsF_6$	3.0	very slow	2.5
$LiClO_4$	2.5	slow	2.1
TEAP	1.5	moderate	1.2
TOAP	1.0	very fast	0.4
$LiBF_4$	3.1	slow	3.0
TEAF	1.5	moderate	1.4
TBAF	2.2	moderate to fast	1.2

Table III. Computed charge and energy densities for various doped PPP films.

Dopant	Charge Density, C/cm^3	Energy Density, $C\text{-}V/cm^3$
$LiAsF_6$	0.4	1.5
$LiClO_4$	0.1	0.3
TEAP	0.3	0.5
TOAP	2.2	2.2
$LiBF_4$	0.5	1.6
TEAF	2.2	3.3
TBAF	2.7	5.9

FIGURE LEGENDS

1. Cyclic voltammetry of 5 mM biphenyl in 0.10 M TBAF/CH_3CN; sweep rate = 100 mV/s. —— 1st scan; ---2nd scan; ·–·– 3rd scan; ···· 10th scan. Similar voltammetry was observed in other BF_4^- electrolytes ($LiBF_4$, TEAF).

2. Cyclic voltammetry of 5 mM biphenyl in 0.10 M $LiClO_4/CH_3CN$; sweep rate = 50 mV/s. —— 1st scan; ---2nd scan; ·–·– 3rd and succeeding scans. Similar voltammetry was observed in solutions containing the following supporting electrolytes: $LiAsF_6$, TEAP, TPAP, and TOAP.

3. PPP electrodeposition in the pulse mode. Pulse height 0 to +1.8 V; modulation frequency = 0.5 Hz. ——initial; ---30 s; ·–·– 2 min; ···· 5 min; –··–·· 10 min. Solution composition is 5 mM biphenyl in 0.10 TBAF/CH_3CN.

4. Same as Figure 3, except solution is $LiClO_4$ electrolyte. —— initial; ---2 min; ·–·– 5 min; ···· 20 min.

5. Cyclic voltammetry of an approximately 1 micron thick thick PPP film on Pt in 0.10 M TBAF/CH_3CN; film was electrochemically deposited in 0.10 M TBAF/CH_3CN from biphenyl (5 mM). (a) Positive; (b) negative potentials. Potentials vs. the Ag/Ag^+ reference.

6. Cyclic voltammetry (negative potentials) at PPP-modified Pt electrode described in Figure 5. Oxygen concentration approximately 1 mM. O_2 was introduced into the cell solution by exposure to air for 30 min. Sweep rates were 25, 50, 100, and 200 mV/s, as indicated in the Figure.

7. Cyclic voltammetry of an approximately 1 micron thick PPP film cast electrochemically from 5 mM biphenyl in 0.10 M TEAP/CH_3CN; sweep rate = 100 mV/s. (a) Positive potentials; (b) negative potentials.

8. Cyclic voltammetry of an approximately 1 micron thick PPP film electrodeposited (from 5 mM biphenyl) in 0.10 M $LiAsF_6/CH_3CN$; sweep rate = 100 mV/s. (a) Anodic sweep; (b) cathodic sweep.

9. Raman spectrum of PPP film formed electrochemically from biphenyl (5.0 mM) in 0.10 M TBAF/CH_3CN.

10. SEM of PPP film cast electrochemically (from biphenyl, 5 mM) in 0.10 M $LiClO_4/CH_3CN$. Base potential was 0 V; pulse height was +1.8 V vs. Ag/Ag^+. Potential modulation frequency was 0.5 Hz.

11. Same as Figure 10, except solution was 0.10 M TBAF/CH_3CN.

12. Same as Figure 10, except solution was 0.10 M $LiAsF_6/CH_3CN$.

13. SEM photomicrographs of PPP-modified Pt electrodes electroformed at (a) 1.50 V; (b) 1.65V; and (c) +1.80 V vs. Ag/Ag^+. Potential was square wave modulated at 0.5 Hz from a base value of 0 V. Solution was 5.0 mM biphenyl in 0.10 M TBAF/CH_3CN.

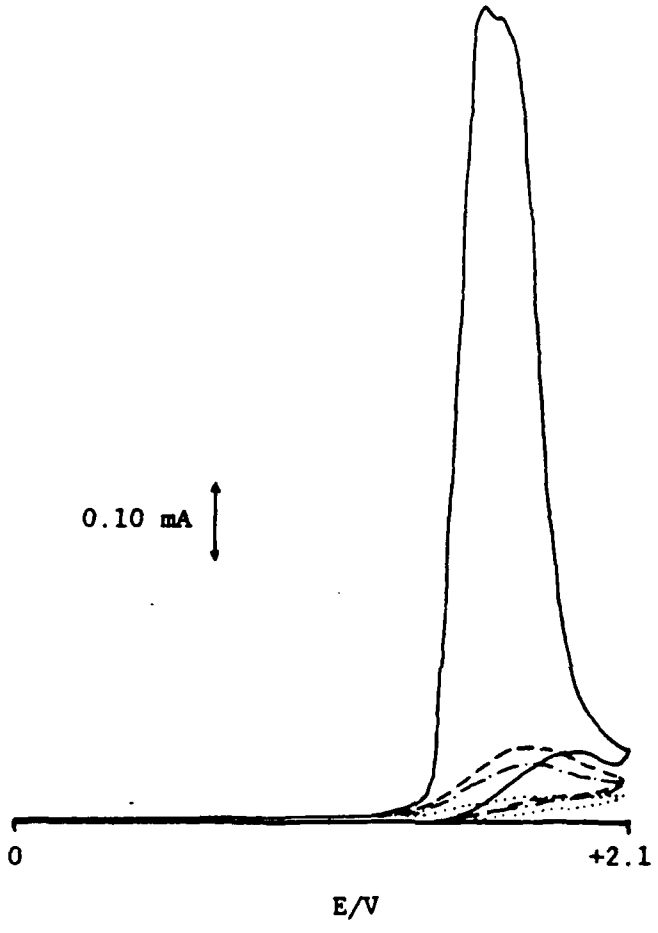

Fig 1

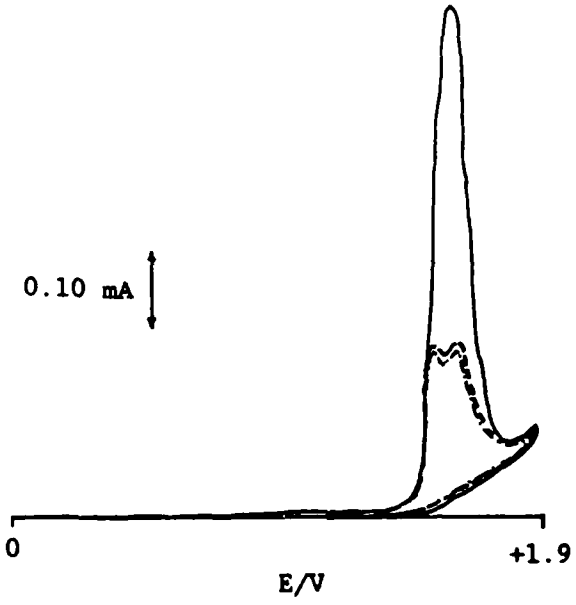

Fig 2

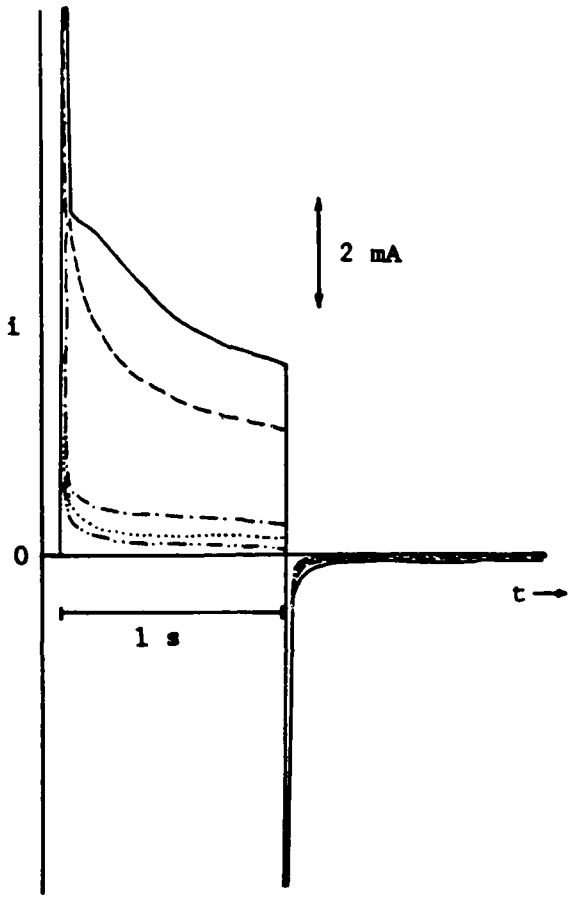

Fig 3

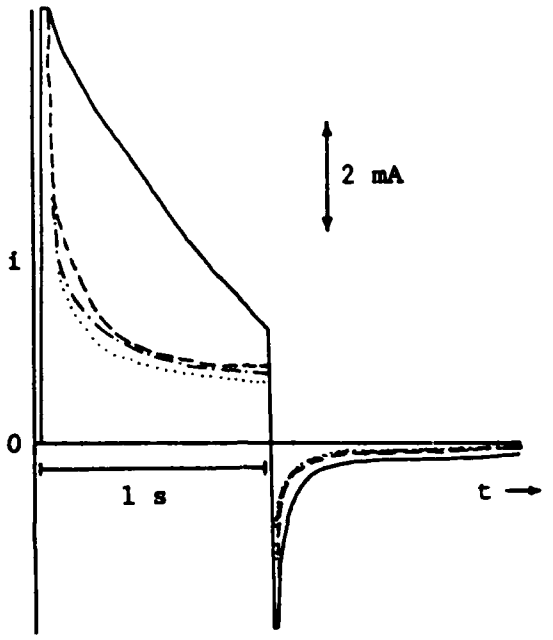

Fig 4

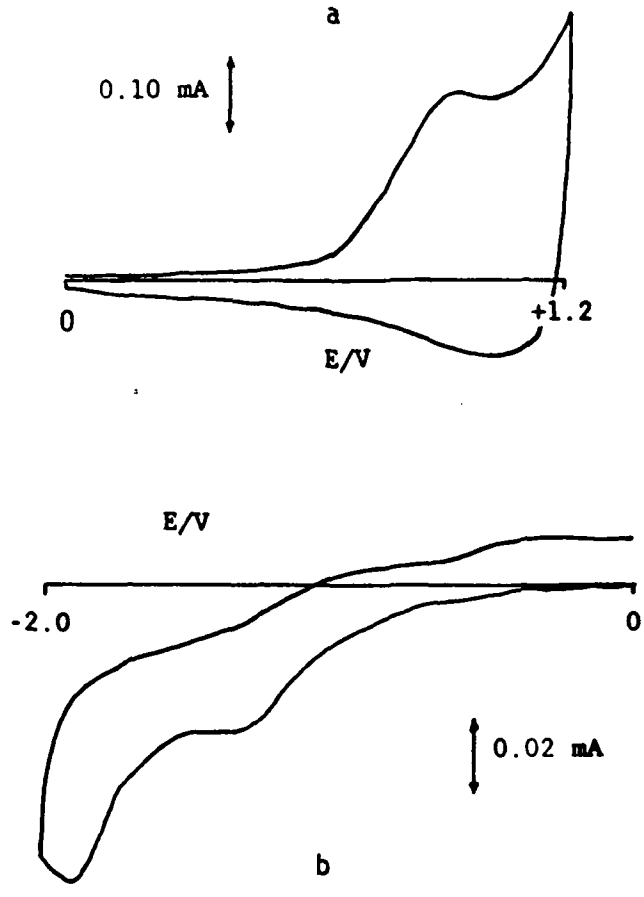

Fig 5

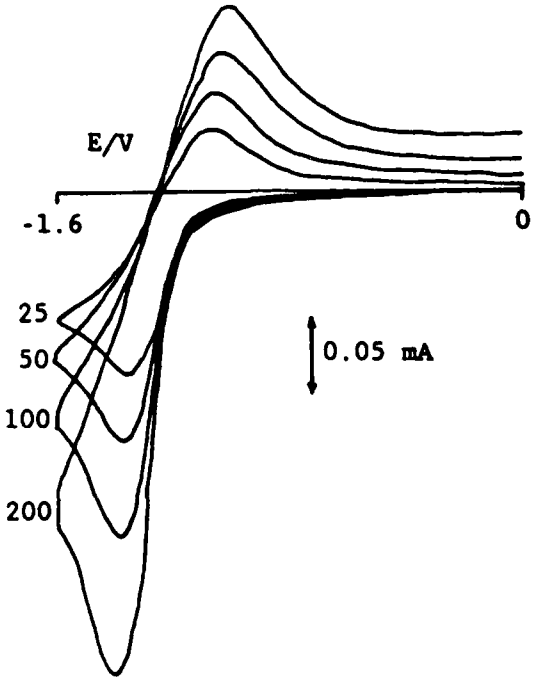

Fig 6

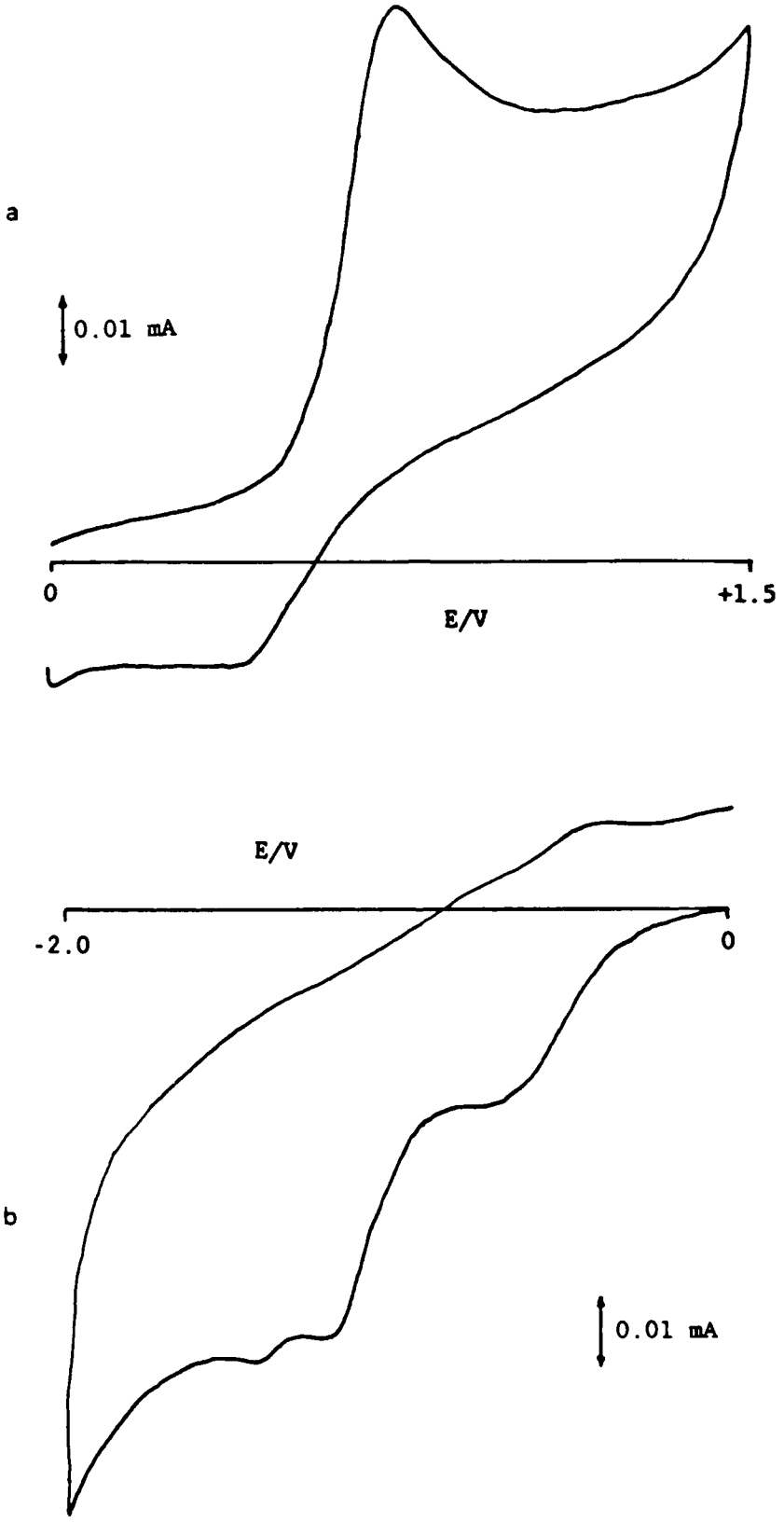

Fig 1

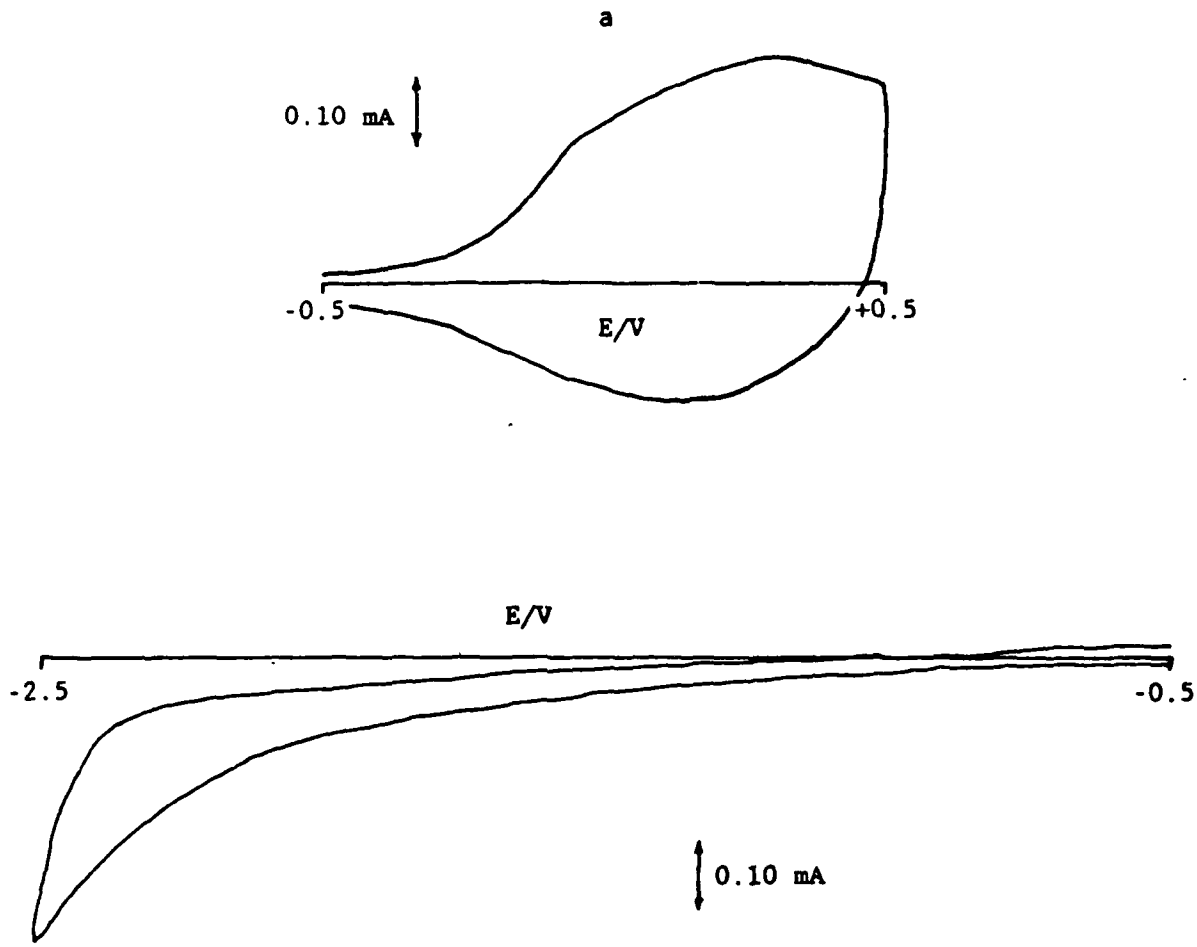

Fig 8

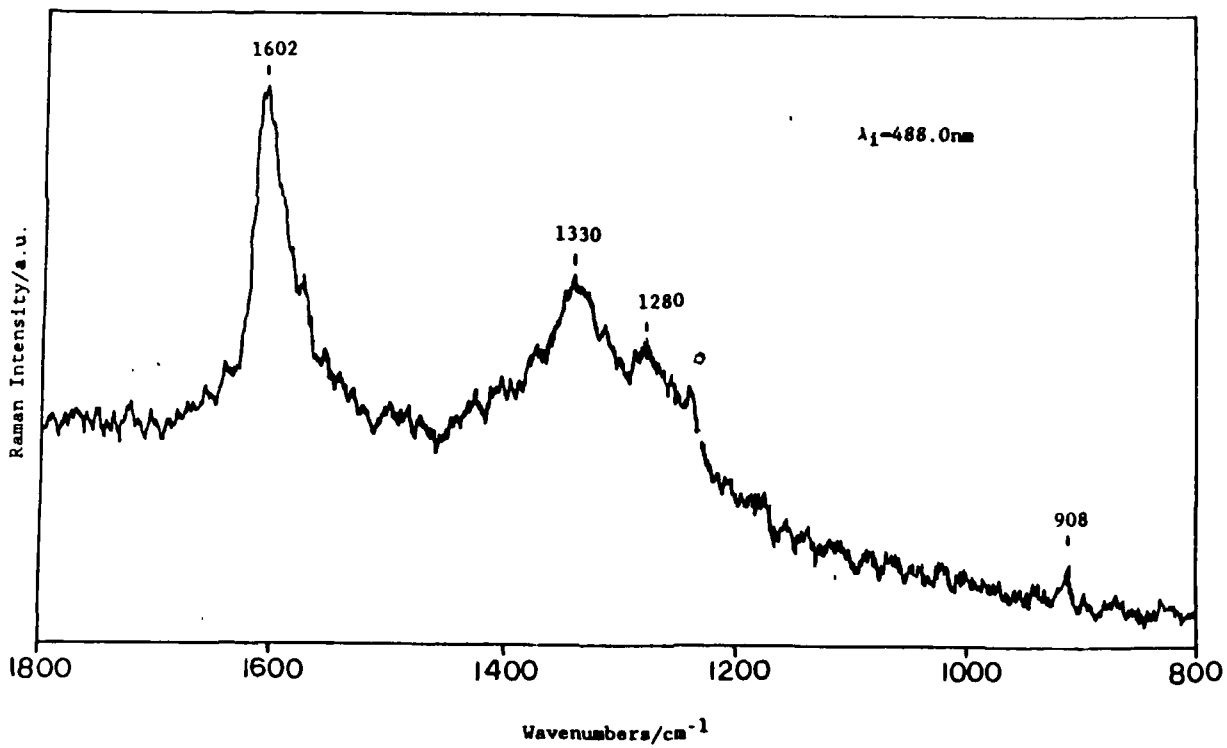
1602
1330
1280
908
λ1=488.0nm
Raman Intensity/a.u.
1800
1600
1400
1200
1000
800
Wavenumbers/cm-1

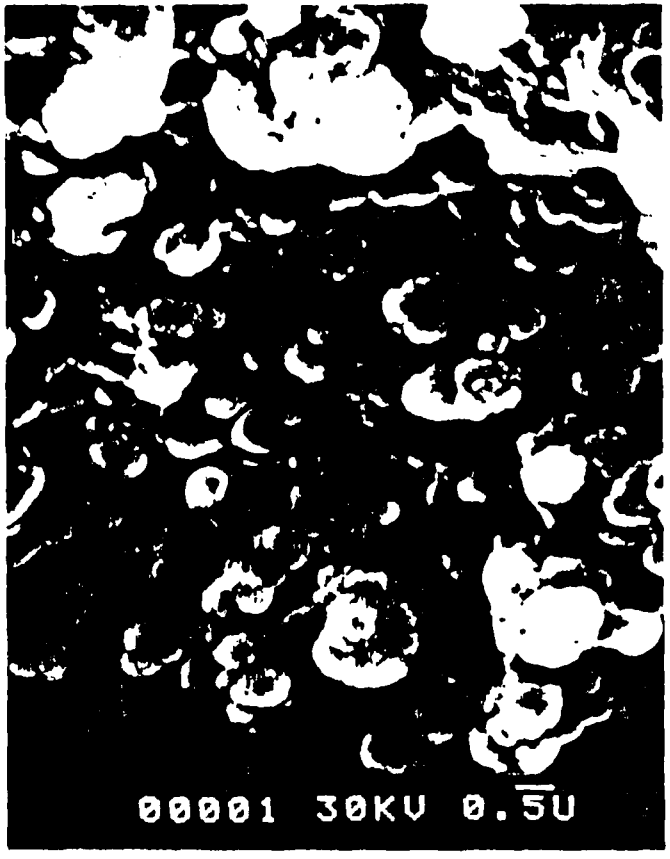

A

B


00001 30KV 0.3U

Please return to author

F.5/12

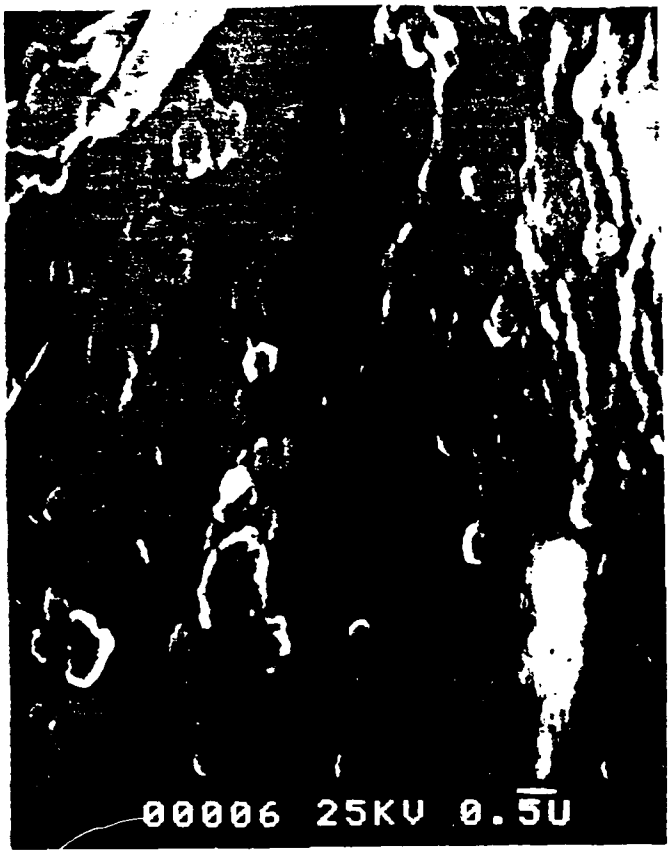

Please return to author

Fig 3

END
DATE
9-88
DTIC